Materials and Structures
DOI 10.1617/s11527-006-9147-3

ORIGINAL ARTICLE

Cement hydration: building bridges and dams at the microstructure level

Dale P. Bentz

Received: 9 March 2005 / Accepted: 31 October 2005

Abstract The concurrent goals of cement hydration are to percolate (bridge) the original cement particles into a load-bearing network and to depercolate (dam) the original water-filled capillary porosity. The initial volume, particle size distribution, and flocculation/dispersion state of the cement particles have a large influence on both hydration rates and microstructure development. Likewise, the capillary porosity as characterized by its pore size distribution, percolation state, and saturation state also influences both hydration kinetics and microstructure. In this paper, experimental techniques and computer modeling are applied to further understanding several of the critical connections between these physical parameters and performance properties. First, the setting or bridging process is explored via a combination of needle penetration and rheological measurements, in concert with three-dimensional microstructural modeling. Second, low temperature calorimetry is shown to be a valuable indicator of the percolation state or damming of the water-filled pores with various size entryways in the three-dimensional microstructure. Porosity percolation (or depercolation) is shown to be strongly influenced by both curing conditions and the alkali content of the cement pastes. Finally, it is proposed that future efforts in this field be directed towards a greater understanding of the (nano)structures of cement hydration products, particularly the calcium silicate hydrate gel, and their influence on performance properties.

Keywords Cement hydration · Low temperature calorimetry · Microstructure · Percolation · Porosity · Rheology · Setting

D. P. Bentz (✉)
Building and Fire Research Laboratory, National Institute of Standards and Technology, Gaithersburg, USA
e-mail: dale.bentz@nist.gov

1 Introduction

As with all materials, the microstructures of cement pastes, mortars, and concretes provide the bridges between materials processing and engineering properties. Unlike many other materials, however, cement-based materials exhibit a highly dynamic (micro)structure that is extremely sensitive to initial conditions, processing, and environmental exposure. There are few materials where water plays such a critical role in processing, microstructure development, performance, and durability. In cement-based materials, water is the liquid that provides flowability to the raw materials, serves as a vehicle for and participant in the numerous and complex cement hydration reactions, exerts forces on the solid components

of the porous microstructure during self-desiccation, drying, freezing, alkali-silica gel formation, and exposure to fire, and provides the pathways for the ingress of deleterious ions. From a geometrical/structural viewpoint, the characteristics of both the **porosity** where the water resides and of the **particles** initially present in the mixing water are critical influences on hydration rates, microstructure, and performance properties. In analogy to large scale construction, cement hydration can be viewed as the process of building *bridges* to connect cement particles and *dams* to disconnect the water-filled capillary pore space.

Because many of the cement hydration products form around the initial cement clinker particles, as shown in Fig. 1, the initial configuration of these particles is crucial in providing a ''scaffold'' on which a network of (porous) solid bridges will form. Thus, the initial water- to-cement ratio (w/c) [1], particle size distribution [2–4], and dispersion/flocculation state [5] of the particles all exert major influences not only on the developed microstructure (through and beyond setting) but also on the hydration kinetics. The bridging process can be conveniently explored via a coordinated experimental and computer modeling approach, as will be demonstrated in this paper.

While the microstructural bridges are critical for strength development and mechanical properties, the microstructural dams are more important for limiting transport and improving the durability of cement-based materials. As cement hydration connects the original cement particles together, it may also disconnect the water-filled capillary porosity, at least at the micrometer scale. Because there are nanometer-sized pores present in the calcium silicate hydrate gel (C–S–H) hydration product, the porosity always remains percolated at the nanometer scale [8]. Although the capillary pores present in both the real and model microstructures in Fig. 1 appear depercolated in two dimensions, in three dimensions, they are still highly connected. But, as first noted by Powers many years ago [9], for lower w/c pastes, sufficient hydration will result in depercolation of the initial water-filled capillary pores. Here, this depercolation, along with the role of curing conditions and cement alkali content, will be examined experimentally using low temperature calorimetry (LTC).

2 Experimental

Cement pastes were prepared using Cement and Concrete Reference Laboratory (CCRL) proficiency cement samples 140 [10] and 152 [11]. Since many of the experimental procedures have been provided in detail elsewhere [12–14], they will only be reviewed briefly here. Cement and water were mixed in a high speed blender using

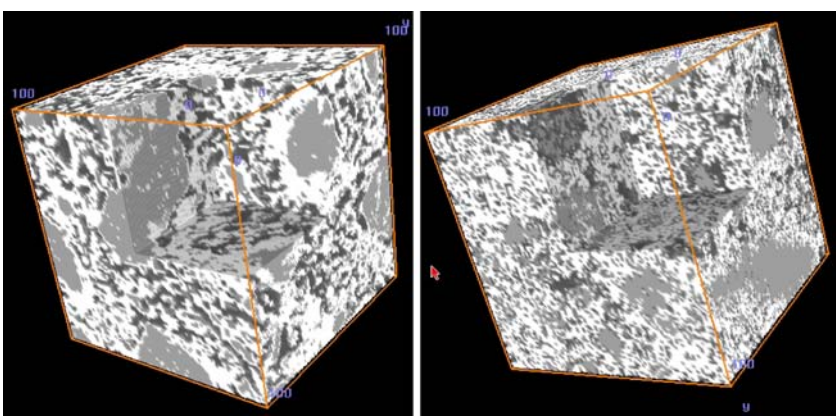

Fig. 1 Greylevel-coded three-dimensional microstructures (100 μm × 100 μm × 100 μm) of real (left) and model (right) hydrating cement pastes of Cement and Concrete Reference Laboratory cement 133 with a w/c≈0.47 and a degree of hydration of about 0.62. Light grey represents unhydrated cement particles, white hydration products, and dark grey capillary porosity. The real microstructure was captured by x-ray microtomography at beam line ID 19 of the European Synchrotron Research Facility in Grenoble, France, in September 2000 [6, 7]

the following protocol: 30 s of low speed mixing while the cement powder is introduced into the mixing vessel that already contains the water, 30 s of high speed mixing, a rest of 150 s while the sides of the mixing vessel are scraped down, and 30 s more of high speed mixing to prepare the final product. The mixing water was either distilled water or a solution of alkalis (sulfates or hydroxides), prepared by dissolving the relevant potassium and sodium compounds in distilled water. The fresh paste was used for Vicat needle penetration [15] measurements at laboratory temperature (about 26°C) and rheological measurements by the stress growth technique [16–18] at 20°C, or cast into small (≈5 g) wafers that were placed in capped plastic vials and cured under saturated (small amount of water on top) or sealed conditions in an environmental chamber maintained at 20°C. Limited repeatability tests have indicated that the calculated values for the yield stress of the cement paste as measured by the stress growth technique have a standard uncertainty of 5% [16–18]. At various ages, the specimens were removed from their vials, crushed using a mortar and pestle, and analyzed using loss-on-ignition (LOI) to assess the degree of hydration and/or LTC to investigate their pore structure. Based on a propagation of error analysis and assuming an uncertainty of 0.001 g in the mass measurements made initially and after heating at 105°C and 1,000°C, the estimated uncertainty in the LOI-calculated degree of hydration was 0.004 [14]. For temperatures between –100 and 500°C, the LTC equipment manufacturer has specified a constant calorimetric sensitivity of ±2.5% and a root-mean-square baseline noise of 1.5 μW.

3 Computer modeling

All simulations were conducted using the CEMHYD3D V3.0 computer programs [19]. Starting microstructures that matched the measured w/c, particle size distribution, phase composition, and phase distribution of cement 152 were created. Because no water-reducing agents were used in the experiment, the digitized spherical cement particles were flocculated, by randomly moving and aggregating together the individual cement particles prior to hydration [5]. Hydration simulations were conducted under sealed conditions and the percolation of the solids was monitored to compare to the physical measurements of setting [20]. During the percolation evaluation, two touching (flocculated) particles are not considered to be connected unless they are bridged by some volume of hydration products, specifically the C–S–H or one of the aluminate hydration products [2, 5, 20]. The volume fractions of the total solids and of the connected solids, defined as those bridging from one side of the microstructure to the opposite one, averaged over the three principal directions, was recorded as a function of hydration cycles. For hydration at 25°C, a conversion factor of 0.00035 h/cycle^2 was used to convert between hydration cycles (squared) and real time [13].

4 Results and discussion

4.1 Bridge building: percolation of solids and setting

Several previous studies have shown a quantitative relationship between setting as measured by the Vicat needle method [15] and the percolation of the solids in a three-dimensional microstructural model [20, 21]. For the standard ASTM technique [15], the Vicat measurements are generally made on a rather low (<0.3) w/c cement paste. It is expected that the setting process would be a strong function of w/c [16–18], as the bridges being constructed to connect the particles together will generally need to be longer and/or fewer bridges per unit hydration of cement will be created when the w/c is increased.

Experimental and computer modeling results examining four different views of the ''setting'' process are provided in Figs. 2, 3. Figure 2 compares experimental measurements of the yield stress via stress growth measurements [16–18] with the computer modeled volume fractions of total solids, both as a function of hydration time for cement pastes with three different w/c (the stress growth measurement technique could not be applied to the w/c = 0.3 cement paste due to its

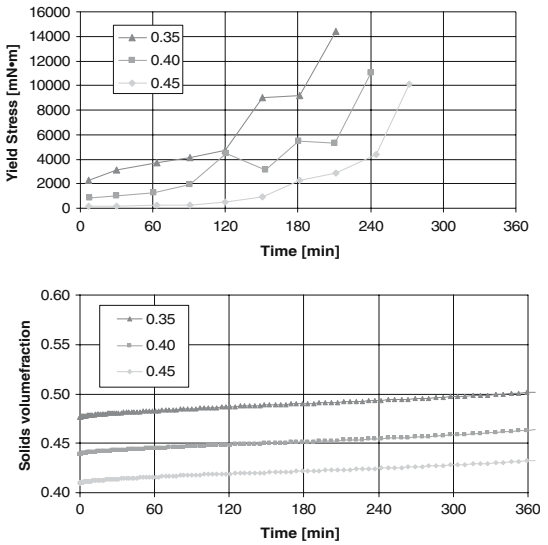

Fig. 2 Two ''views'' of the setting process in cement paste as a function of w/c: yield stress by stress growth measurements (top) and total solids volume fraction (bottom)

high initial stiffness). As the cement particles flocculate together following mixing, they form a weak solid skeleton that is strengthened and reinforced by the cement hydration products. For a high enough w/c, this initial skeleton cannot support itself under gravity so that settlement and bleeding will occur. In fact, minor bleeding was

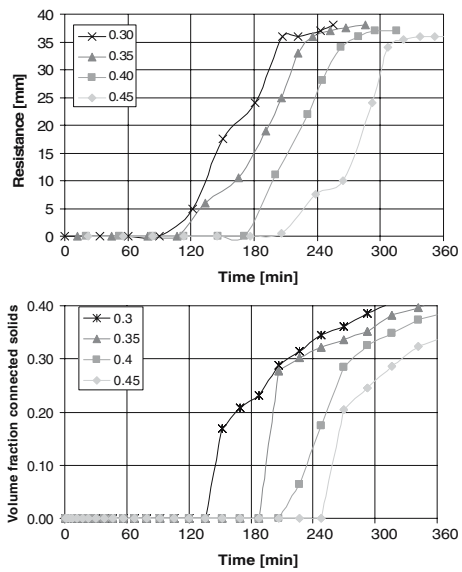

Fig. 3 Two more ''views'' of the setting process in cement paste as a function of w/c: needle resistance (top) and connected solids volume fraction (bottom)

observed for the w/c = 0.45 cement paste prepared with CCRL cement 152, and the initial yield stress values in Fig. 2 are quite low. As the w/c is lowered to 0.4 and then to 0.35, the measured yield stress becomes higher as a greater applied stress is necessary to get the (greater number of) particles moving in the more concentrated suspensions. Initially, the model-predicted solids volume fraction and the measured yield stress track each other fairly closely, but for each w/c ratio, a point is reached where the measured yield stress climbs rapidly while the modeled volume fraction of solids continues to increase at a relatively constant and much slower rate. It is here that the percolation of the partially hydrated cement particles by the hydration products comes into play.

The bridges built by the hydration products are much stronger than the initial interparticle forces flocculating the particles together. As these bridges percolate the three-dimensional microstructure, a finite resistance to the penetration of the Vicat needle is developed, as shown in Fig. 3. The time at which the needle resistance, equal to (40 mm – the needle penetration in mm), begins to increase from zero in Fig 3 is seen to correspond closely to the time when the measured yield stress begins to diverge in Fig. 2. In Fig. 3, the needle resistance measurements are seen to also be in general agreement with the modeled volume fraction of connected solids that characterizes the volume fraction of unhydrated cement clinker particles that are bridged by hydration products. All of this has occurred during the time when only the first 4–8% of the cement has hydrated. Already at this point, the solid skeleton is well in place and the strength of the microstructure will continuously increase as new bridges are formed and existing ones are expanded.

4.2 Dam building: depercolation of capillary porosity and influences of curing conditions and cement alkali content

While Powers first inferred depercolation of the capillary porosity in hydrating cement paste via measurements of permeability [9], the depercolation can also be observed based on chemical shrinkage measurements on pastes of various

thicknesses [22] or via low temperature calorimetry scans [23–25]. A cooling scan in an LTC experiment is basically equivalent to a mercury porosimetry intrusion scan [23], but with the advantage that no drying of the specimen is required. Generally, a percolated water-filled capillary pore structure is indicated by a peak around –15°C [25]. Thus, the presence or absence of this peak can be used to infer a percolated or depercolated capillary pore structure, respectively.

Figure 4 provides representative LTC scans of a w/c = 0.35 cement paste cured under saturated or sealed conditions, along with scans on the pastes cured under sealed conditions after 24 h or more of resaturation. The w/c = 0.35 is low enough that depercolation of the capillary pores would be expected to occur during the first week of curing [9]. For the various scans in Fig. 4, basically three different peaks are observed corresponding to percolated capillary pores (freezing at about –15°C), open gel pores (freezing at –25°C to –30°C), and dense gel pores (freezing at –40°C to –45°C) as defined in [25]. For saturated curing, the capillary pores are observed to depercolate between 3 d and 4 d of curing. Initially, a similar depercolation is observed for the capillary pores in the specimens exposed to sealed curing conditions. After a few weeks of curing, the open gel pores generally also depercolate, so that only pores accessible via the dense gel pores are detected via LTC. Specimens cured under sealed conditions are consistently seen to have smaller peaks for the capillary and open gel pores, as these larger pores are the first to empty due to chemical shrinkage and self-desiccation [12, 26].

Interestingly, resaturation of the sealed specimens reveals a change in the percolation of the capillary pores that is not observed for the specimens cured under saturated conditions. For sealed conditions, while the capillary pores do initially depercolate, by 14 d, when resaturated, the specimens exhibit a repercolated set of capillary pores (bottom plot for Fig. 4), most likely due to the autogenous stresses and strains placed on the three-dimensional microstructure due to self-desiccation [26]. Similar effects have been observed by Bager and Sellevold upon exposing well-hydrated cement pastes to drying/resaturation [23]. Drying, whether external or internal (self-desiccation), results in the creation of a percolated set of capillary pores (or perhaps microcracks). As shown by the scanning electron micrographs in Fig. 5, the specimens cured under sealed conditions definitely contain a set of large capillary pores relative to those present in the paste specimens cured under saturated conditions. Thus, a plausible explanation for the behavior observed for the sealed/resaturated specimens is that the autogenous shrinkage of the C–S–H gel reopens the entryways of the previously depercolated capillary pore network. Still, it cannot be ruled out that some microcracks could

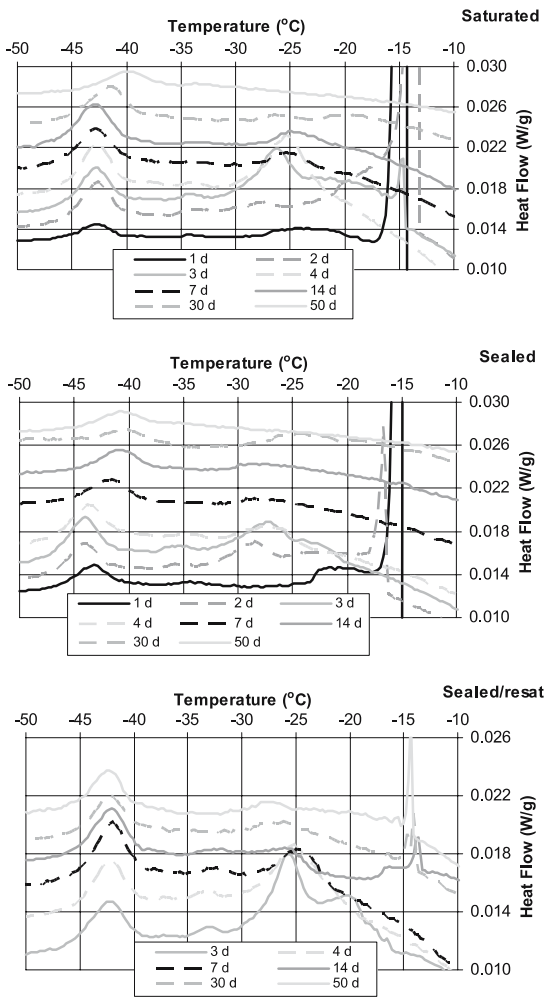

Fig. 4 LTC results for CCRL cement 152 specimens (w/c = 0.35, 20°C) at various ages, cured under saturated (top) and sealed (middle) conditions and for specimens cured under sealed conditions for the indicated number of days and then resaturated (bottom) [12]

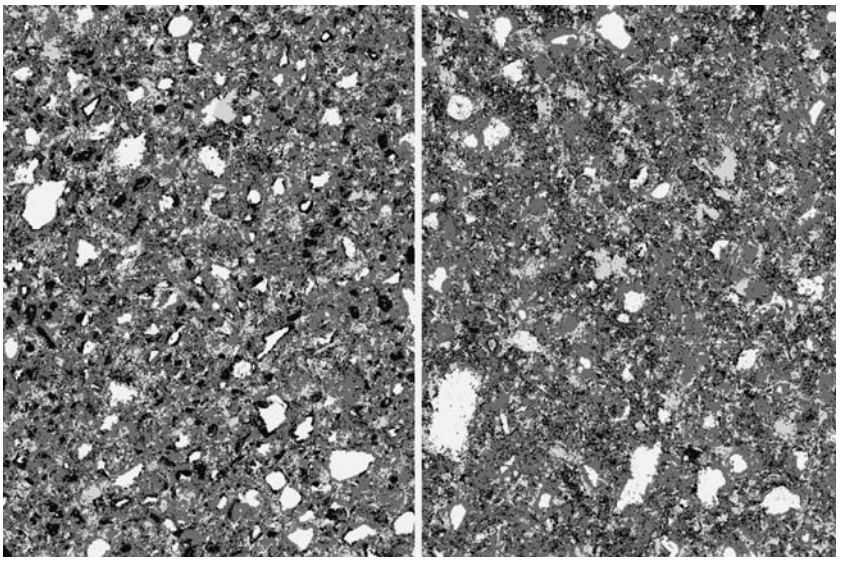

Fig. 5 Ninety-two day (92 d) segmented scanning electron microscopy (SEM) images for CCRL cement 152, w/c = 0.35 cement paste specimens cured under sealed (left) and saturated (right) conditions [12]. Unhydrated cement particles are white, calcium hydroxide is light grey, C–S–H and other hydration products are dark grey, and capillary pores are black. Images are 384 μm by 512 μm

also participate in either repercolating the capillary pores or creating their own percolated network of porosity.

While sealed curing appears to be detrimental in terms of microstructure (specifically pore structure) development for w/c = 0.35 pastes, for w/c = 0.435 pastes, as illustrated by the LTC cooling scans in Fig. 6, it may actually be beneficial. As self-desiccation occurs during sealed curing, the largest water-filled pores in the three-dimensional microstructure will empty first [12, 26]. Since cement hydration products will generally not precipitate and grow in air (or water vapor)-filled pores, hydration product formation will tend to be concentrated in the remaining smaller pores and pore entryways, where it should be more effective in depercolating the (water and vapor-filled) capillary pores [12], as supported by the experimental results in Fig. 6. Thus, if curing to minimize transport and maximize durability, for an intermediate range of w/c (e.g., 0.4–0.45), some type of sealed/saturated curing could be superior to maintaining saturated conditions throughout. Such a seemingly counterintuitive concept is not new, having been suggested by both Swayze [27] and Powers [28] over 50 years ago.

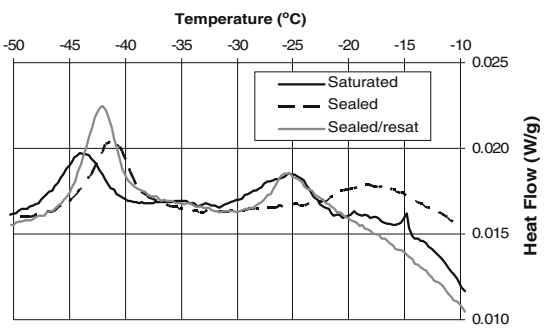

Fig. 6 LTC results for CCRL proficiency cement 152 specimens (w/c = 0.435, 20°C) cured for 214 d [12]

Recently, it has been demonstrated that the percolation of the capillary porosity in hydrating cement paste can also be influenced by the level of alkalis in the cement paste [12, 14]. In the presence of sufficient alkali ions, the C–S–H has a tendency to form lath or plate-like nanostructures, with a higher degree of crystallinity [29]. Simple three-dimensional microstructure models have indicated that hydration products forming as needles or plates, as opposed to a random geometry, can be more efficient at depercolating the capillary pore space between the original cement particles [14]. In Fig. 7, LTC cooling scans are provided for a set of hydrated cement pastes with and without additional alkalis, all of which have achieved nominally the same degree of hydration after 8 d of curing at 20°C [14]. While the paste with no additional alkalis clearly contains both percolated capillary and open gel pore structures, only dense gel pores are identified in the pastes with either alkali sulfate or alkali hydroxide additions. For both additions, the same

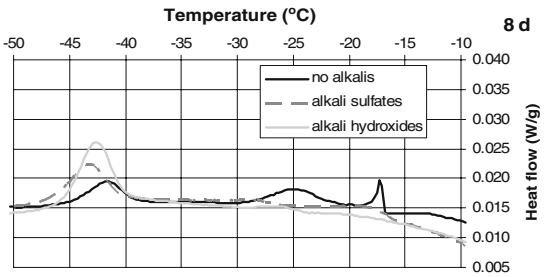

Fig. 7 LTC results for CCRL cement 140 specimens (w/c = 0.40, hydrated under saturated conditions for 8 d at 20°C) with and without alkali additions (sulfates or hydroxides) [14]. All specimens have achieved basically the same degree of hydration, as measured using LOI [14]

molar quantities of potassium and sodium ions (per unit mass of cement) were added to the mixing water and dissolved completely prior to the addition of the cement. This example illustrates one potential method for engineering the nanostructure of the dams formed during cement hydration.

4.3 Prospectus for future research – migration from microstructure to nanostructure

In the future, the research focus will likely move from the microstructure created by the bridges and dams to the nanostructure of the bridges and dams themselves. For example, silica fume has a significant influence on the nanostructure of the dams, as illustrated by its large (up to 25×) influence on transport through the C–S–H gel [30]. As shown above, alkalis also definitely influence the nanostructure and crystallinity of the C–S–H gel. The nanostructure of the C–S–H gel is already being extensively studied, and atomic and nanostructure-level models are being advanced [29, 31, 32]. The ultimate engineering of the microstructure of cement-based materials will reach fruition only when the nanostructures of the bridges and dams comprising its building blocks are understood and predictable.

5 Conclusions

The construction of microstructural bridges and dams within hydrating cement paste has been investigated using a coordinated experimental/computer modeling approach. Bridge building is seen to be critical for the setting process, and of course also for the subsequent development of strength and mechanical properties. On the other hand, dam building is critical in depercolating the capillary porosity, leading to reduced transport coefficients and hopefully enhanced durability. Opportunities for engineering not only the nanostructure of the bridges and dams but also how they assemble at the microstructure level exist and will surely lead to innovative new materials and structures.

Acknowledgements The author would like to thank Dr. Chiara Ferraris and Mr. John Winpigler of BFRL/NIST for obtaining and processing the needle penetration and rheological data presented in this paper.

References

1. Bentz DP (2006) Influence of water-to-cement ratio on hydration kinetics: simple models based on spatial considerations. Cem Concr Res 36:238–244
2. Bentz DP, Garboczi EJ, Haecker CJ, Jensen OM (1999) Effects of cement particle size distribution on performance properties of cement-based materials. Cem Concr Res 29:1663–1671
3. Knudsen T (1984) The dispersion model for hydration of portland cement 1. General concepts. Cem Concrete Res 14:622–630
4. Osbaeck B, Johansen V (1989) Particle size distribution and rate of strength development of portland cement. J Am Cer Soc 72(2):197–201
5. Bentz DP, Garboczi EJ, Martys NS (1996) Application of digital-image-based models to microstructure, transport properties, and degradation of cement-based materials. In: Jennings HM et al. (eds) The modelling of microstructure and its potential for studying transport properties and durability. Kluwer Academic Publishers, pp 167–186
6. Bentz DP, Mizell S, Satterfield S, Devaney J, George W, Ketcham P, Graham J, Porterfield J, Quenard D, Vallee F, Sallee H, Boller E, Baruchel J (2002) The visible cement data set. J Res Natl Inst Stand Technol 107(2):137–148
7. Bentz DP (2006) Quantitative comparison of real and CEMHYD3D model microstructures using correlation functions. Cem Concr Res 36:259–263
8. Holzer L, Gasser Ph, Münch B (2005) Three Dimensional Analysis of the Pore-Network in Cement Pastes Using FIB-Nanotomography. Int. Conf. Cementitious Materials as Model Porous Media: Nanostructure and Transport. Verita, Switzerland, pp. 71–76
9. Powers TC (1959) Capillary continuity or discontinuity in cement paste. PCA Bull 10:2–12

10. Cement and Concrete Reference Laboratory (2001) Cement and concrete reference laboratory proficiency sample program: final report on portland cement proficiency samples number 139 and 140. Gaithersburg, MD
11. Cement and Concrete Reference Laboratory (2004) Cement and concrete reference laboratory proficiency sample program: final report on portland cement proficiency samples number 151 and 152. Gaithersburg, MD, April available at http://www.ccrl.us
12. Bentz DP, Stutzman PE (2006) Curing, hydration, and microstructure of cement paste. ACI Mater J (accepted)
13. Bentz DP (2006) Modeling the influence of limestone filler on cement hydration using CEMHYD3D. Cem Concr Compo 28:124–129
14. Bentz DP (2006) Influence of alkalis on porosity percolation in hydrating cement pastes. Cem Concr Compo 28:427–431
15. ASTM C191-04b (2004) Standard Test Method for Time of Setting of Hydraulic Cement by Vicat Needle. ASTM Annual Book of Standards, vol 04.01 (Cement; Lime; Gypsum) American Society for Testing and Materials, West Conshohocken, PA
16. Amziane S, Ferraris CF (2005) Monitoring of setting evolution of cementitious materials by measurements of rheological properties and hydraulic pressure variations. ACI Mater J (submitted)
17. Amziane S, Ferraris CF (2005) SCC evolution of formwork hydraulic pressure and rheological properties. ACI Proc, New York
18. Amziane S, Ferraris CF (2004) Caractérisation de la prise des matériaux cimentaires. Proc. of the GFR convention, Mulhouse (France) October (in French)
19. Bentz DP (2005) CEMHYD3D: a three-dimensional cement hydration and microstructure development modelling package. Version 3.0. NISTIR 7232, U.S. Department of Commerce, June
20. Haecker CJ, Bentz DP, Feng XP, Stutzman PE (2003) Prediction of cement physical properties by virtual testing. Cem Int 1(3):86–92
21. Principallo A, Lura P, van Breugel K, Levita G (2003) Early development of properties in a cement paste: a numerical and experimental study. Cem Concr Res 33:1013–1020
22. Geiker M (1983) Studies of portland cement hydration: measurement of chemical shrinkage and a systematic evaluation of hydration curves by means of the dispersion model. Ph.D. Thesis, Technical University of Denmark, Lyngby, Denmark
23. Bager DH, Sellevold EJ (1986) Ice formation in hardened cement paste, Part II- Drying and resaturation on room temperature cured pastes. Cem Concr Res 16:835–844
24. Villadsen J (1989) Hærdetemperaturens indflydelse på hærdnet cementpastas porestruktur: projektrapport. The Technical University of Denmark, Lyngby, Denmark
25. Snyder KA, Bentz DP (2004) Suspended hydration and loss of freezable water in cement pastes exposed to 90% relative humidity. Cem Concr Res 34(11):2045–2056
26. Bentz DP, Jensen OM, Hansen KK, Oleson JF, Stang H, Haecker CJ (2001) Influence of cement particle size distribution on early age autogenous strains and stresses in cement-based materials. J Am Ceram Soc 84(1):129–135
27. Swayze MA (1942) Early concrete volume changes and their control. J Am Concr Inst 13(5):425–440
28. Powers TC (1947) A discussion of cement hydration in relation to the curing of concrete. Proc Highway Res Board 27:178–188
29. Richardson IG (2004) Tobermorite/jennite- and tobermorite/calcium hydroxide-based models for the structure of C–S–H: applicability to hardened pastes of tricalcium silicate, β-dicalcium silicate, portland cement, and blends of portland cement with blast-furnace slag, metakaolin, or silica fume. Cem Concr Res 34:1733–1777
30. Bentz DP, Jensen OM, Coats AM, Glasser FP (2000) Influence of silica fume on diffusivity in cement-based materials. I. Experimental and computer modeling studies on cement pastes. Cem Concr Res 30:953–962
31. Nonat A, (2004) The structure and stoichiometry of C–S–H. Cem Concr Res 34:1521–1528
32. Cong X, Kirkpatrick RJ (1996) ^{29}Si MAS NMR study of the structure of calcium silicate hydrate. Adv Cement-Based Mater 3:144–156